# Mechanism for linear and nonlinear optical effects in $LiB_3O_5$, $CsB_3O_5$, and $CsLiB_6O_{10}$ crystals

Zheshuai Lin, Jiao Lin,* Zhizhong Wang, and Chuangtian Chen
*Beijing Center for Crystal Research & Development, Chinese Academy of Sciences, P.O. Box 2711, Beijing, 100080, China*

Ming-Hsien Lee
*Department of Physics, Tamkang University, Tamsui, Taipei 251, Taiwan*
(Received 28 January 2000)

Electronic structure calculations of $LiB_3O_5$, $CsB_3O_5$, and $CsLiB_6O_{10}$ crystals from first principles are performed based on a plane-wave pseudopotential method. The static second-harmonic generation (SHG) coefficients are calculated at the independent-particle level with a formalism improved by our group and co-workers [Phys. Rev. B **60**, 13 380 (1999)]. A real-space atom-cutting method is adopted to analyze the respective contributions of the cation and anionic groups to optical response. The calculated refractive indices and SHG coefficients are in good agreement with the experimental values. On the basis of these calculations, the influence of the cations on the band gaps and the optical responses is evaluated. The results show that with the increase of their radius their contributions to SHG become slightly more pronounced.

## I. INTRODUCTION

Recently, we have employed CASTEP,[1] a plane-wave pseudopotential total-energy package, to calculate the electronic band structure and linear and nonlinear optical properties of $BaB_2O_4$ (BBO) with the local-density approximation[2] (LDA) based on density-functional theory.[3] In the meantime, a real-space atom-cutting method has been suggested to analyze the respective contributions of various transitions among cations and anionic groups to the optical response of the BBO crystal.[4] The results indicate that although the $Ba^{2+}$ cations make a contribution to the refractive index (about 10%) and second-harmonic generation (SHG) coefficient (about 15%), the major contribution to the SHG coefficient, refractive index, and birefringence, in particular for BBO, comes from the $(B_3O_6)^{3-}$ anionic group. In this paper, we will use the same calculation methods to analyze the mechanism for the linear and nonlinear optical properties of $LiB_3O_5$ (LBO), $CsB_3O_5$ (CBO) and $CsLiB_6O_{10}$ (CLBO).

LBO and CBO were discovered, respectively, by Chen and co-workers[5,6] and Wu *et al.*[7] on the basis of the anionic group theory[5] during 1987 to 1993.[6,7] Meanwhile, CLBO was first discovered in 1995 by Tu and Kaszler[8] and Mori *et al.*[9] independently. The discovery of these new borate series nonlinear optical (NLO) crystals after BBO greatly promoted the development of green-ultraviolet laser systems. Recently, LBO has become a major NLO crystal to produce high-power green laser light and CLBO is one of the most promising crystals for 266-nm coherent radiation. Although the mechanism of producing SHG in LBO and CBO can be understood on the basis of the anionic group theory,[5] a more comprehensive understanding can only be achieved by performing the *ab initio* energy band-structure calculation, in which the influence of cations on the band gap and optical response with the increasing radius of the cations can be directly evaluated.

French *et al.* first used the discrete-variational self-consistent multipolar $X\alpha$ (DV-SCM-$X\alpha$) method, VUV spectroscopy, and valence-band x-ray photoemission spectroscopy (XPS) to investigate the valence-band density of states in LBO crystal.[10] The results indicate that the large band gap and transparency region of LBO arise from two factors, the linkage of the anionic groups in the crystal and reduced $\pi$-conjugated bonding in the borate anionic groups. These structural characteristics are quite different from that of BBO, in which $(B_3O_6)^{3-}$ anionic groups are isolated and contain $\pi$-conjugated orbitals. Xu and Ching[11] and Xu, Ching, and French[12] were the first to use the first-principles orthogonalized linear combination of atomic orbitals (OLCAO) method to study the electronic structures and optical properties of LBO and BBO. They indicated that the band gap and linear optical properties of LBO are determined by the microstructure of the $(B_3O_7)^{5-}$ group. Li and co-workers have published a first-principles calculation of the electronic structure and linear optical properties of LBO, CBO, and BBO crystals by means of the linearized argumented plane-wave band method.[13–15] They pointed out that the top of the valence band mainly consists of O orbitals, while the bottom of the conduction bands for LBO consists of trigonal coordinated B-O bonds. However, the bottom of the conduction bands for CBO consists mainly of cation states. Up to now in the literature, there has been no calculation on the electronic band structure of the CLBO crystal.

In this article we present a systematic study on the mechanism of linear and NLO optical effects in LBO, CBO, and CLBO crystals based on the local-density approximation[2] with the CASTEP package.[1] We first determined the band structures of LBO, CBO, and CLBO crystal with the CASTEP program. Second, the refractive indices, birefringence, and SHG coefficients of the above-mentioned crystals were calculated from their band structures. Third, a real-space atom-cutting method developed by our group[4] was used to analyze quantitatively the respective contributions of cations and anionic groups to the various optical properties. This information is essential to the design and search for new NLO crystals. Finally, several useful results are given.

 

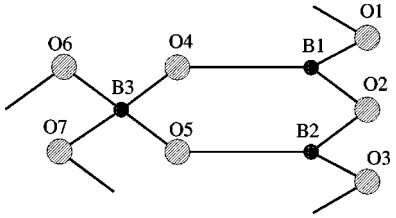


FIG. 1. The $(B_3O_7)^{5-}$ anionic group.

## II. METHODS AND COMPUTATIONAL DETAILS

CASTEP,[1] a plane-wave psuedopotential total-energy package, is used for solving the electronic and band structures as well as linear and nonlinear optical properties of LBO, CBO, and CLBO crystals. The theoretical basis of CASTEP is the density-functional theory[3] in the local-density approximation[2] or gradient-corrected LDA developed by Perdew and Wang.[16] Within such a framework, the preconditioned conjugated gradient (CG) band-by-band method[17] used in CASTEP ensures a robust and efficient search of the energy minimum of the electronic structure ground state. The optimized pseudopotential[18–20] in the Kleinman-Bylander form[21] for Li, Cs, B, and O allows us to use small plane-wave basis sets without compromising the accuracy required by our study.

It is well known that the band gap calculated by the LDA is usually smaller than the experimental data. A scissors operator[22,23] is also used to shift all the conduction bands in order to agree with measured values of the band gap.

We have reviewed the calculation methods for SHG coefficients.[4] The static limit of the SHG coefficients plays the most important role in the application of SHG crystals, so we adopt the formula presented by Rashkeev, Lambrecht, and Segall[24] and improved by us,[4]

$$\chi^{\alpha\beta\gamma}=\chi^{\alpha\beta\gamma}(\mathrm{VE})+\chi^{\alpha\beta\gamma}(\mathrm{VH})+\chi^{\alpha\beta\gamma}(\text{two band}),$$

where $\chi^{\alpha\beta\gamma}(\mathrm{VE})$ and $\chi^{\alpha\beta\gamma}(\mathrm{VH})$ give the contributions to $\chi_i^{(2)}$ from virtual-electron processes and virtual-hole processes, respectively; $\chi^{\alpha\beta\gamma}(\text{two band})$ is the contribution to $\chi_i^{(2)}$ from the two-band processes. The formula for calculating $\chi^{\alpha\beta\gamma}(\mathrm{VE})$, $\chi^{\alpha\beta\gamma}(\mathrm{VH})$, and $\chi^{\alpha\beta\gamma}(\text{two band})$ are given in Ref. 4.

The parameters of LBO, CBO, and CLBO are as follows: LBO ($a=8.46$ Å, $b=5.13$ Å, $c=7.38$ Å, $\alpha=\beta=\gamma=90°$),[25] CBO ($a=6.21$ Å, $b=8.521$ Å, $c=9.17$ Å, $\alpha=\beta=\gamma=90°$),[26] and CLBO ($a=b=10.494$ Å, $c=8.939$ Å, $\alpha=\beta=\gamma=90°$).[27] Their unit cells contain 36, 36, and 72 atoms, respectively. In the above space structures LBO and CBO belong to the orthorhombic, with space group $Pn2_1a$ (Ref. 24) and $P2_12_12_1$ (Ref. 25), respectively, and contain four formula units, i.e., 36 atoms in one unit cell, while CLBO is a tetragonal crystal with space group $I$-$42d$. The basic structures of these crystals are built up with a continuous network of $(B_3O_7)^{5-}$ groups, which is shown in Fig. 1. In the figure, B1 and B2 are trihedrally coordinated, where B3 is tetrahedrally coordinated; O1, O3, O6, and O7 are exocyclic; O2, O4, and O5 are in the ring. Because of bridging of the tetrahedrally coordinated B, the $(B_3O_7)^{5-}$ anion groups are linked to each other to form an endless network in three crystals, with cations located in the interstices to give the whole structure neutralization. This arrangement is different from layer-stacked BBO with $(B_3O_6)^{3-}$ as the structure unit. All these factors should have their specific influence on the electronic structures of LBO, CBO, and CLBO, and consequently on their optical properties. An *ab initio* psuedopotential band calculation can reveal the effects in a straightforward manner. With a real-space atom-cutting method, the respective actions of the anionic group and cations ($Li^+$ and $Cs^+$) on the optical properties may be recognized and understood. This is the goal of the present paper.

## III. RESULTS AND DISCUSSIONS

### A. The band structures

The calculated band structures of LBO, CBO, and CLBO in the unit cell are plotted along the symmetry lines in Figs. 2(a), 2(b), and 2(c), respectively. Obviously, each energy band can be divided into three regions. The lower region lies below $-15$ eV, and mainly consists of $2s$ orbitals of oxygen atoms. The middle region is the valence band (VB) from about $-9$ to 0 eV. The upper one is the conduction band (CB). Although the three crystals considered have different symmetry, their valence bands are very flat and qualitatively similar to each other. The apparent difference occurs at the bottom of their conduction bands, in which a band of large dispersion spanning about 1 eV appears in CBO and CLBO. The calculated band gaps of LBO, CBO, and CLBO are 4.825, 4.463, and 4.321 eV, respectively. These theoretical values from the density-functional theory are all smaller than corresponding experimental data (see Table I), the error being due to the discontinuity of the exchange-correlation energy. Moreover, we have tried to use the other kinds of psuedopotentials to calculate the bands and found that the change of the results is not apparent. For LBO and CBO, our energy-band profiles are qualitatively similar to those obtained by Li *et al.*[13]

Figures 3(a), 3(b), and 3(c) give the total density of states (DOS) and partial DOS (PDOS) projected on the constitutional atoms of LBO, CBO, and CLBO crystals, respectively. As an example, Figs. 4(a), 4(b), and 4(c) show the orbital-resolved PDOS of Cs, O, and B in CBO crystal, respectively. Obviously, several characteristics can be seen from the DOS and PDOS figures. (1) The orbitals of the lithium atoms have no contributions to the entire bands of LBO and CLBO. (2) The bands lower than $-15$ eV mostly consist of $2s$ orbitals of both ring and exocyclic oxygen atoms (see Fig. 1), but for CBO and CLBO there is a little mixing of the $6s$ orbital of Cs. In fact, the $2s$ orbitals of the oxygen atoms are strongly localized at $-17$ eV. (3) The valence bands are all composed of $2p$ orbitals of both ring and exocyclic oxygen atoms, but for CBO and CLBO there are strong contributions from the $6p$ orbitals of Cs, which are located at $-5.5$ eV. These PDOS figures show that at the very top of the VB (from 0 to $-3$ eV), there is no obvious hybridization between B and O atoms, but there is a mixture of $p$ orbitals of both ring and exocyclic oxygen atoms. This conclusion is in agreement with that of Li *et al.*[13] (4) The conduction bands of the three crystals are mainly composed of valence orbitals of O and B. Furthermore, for the CBO crystal there are apparent contributions from the $d$ orbitals of the Cs atom [see Figs. 3(b) and 4(a)]. (5) Experiments show that from LBO to CLBO the

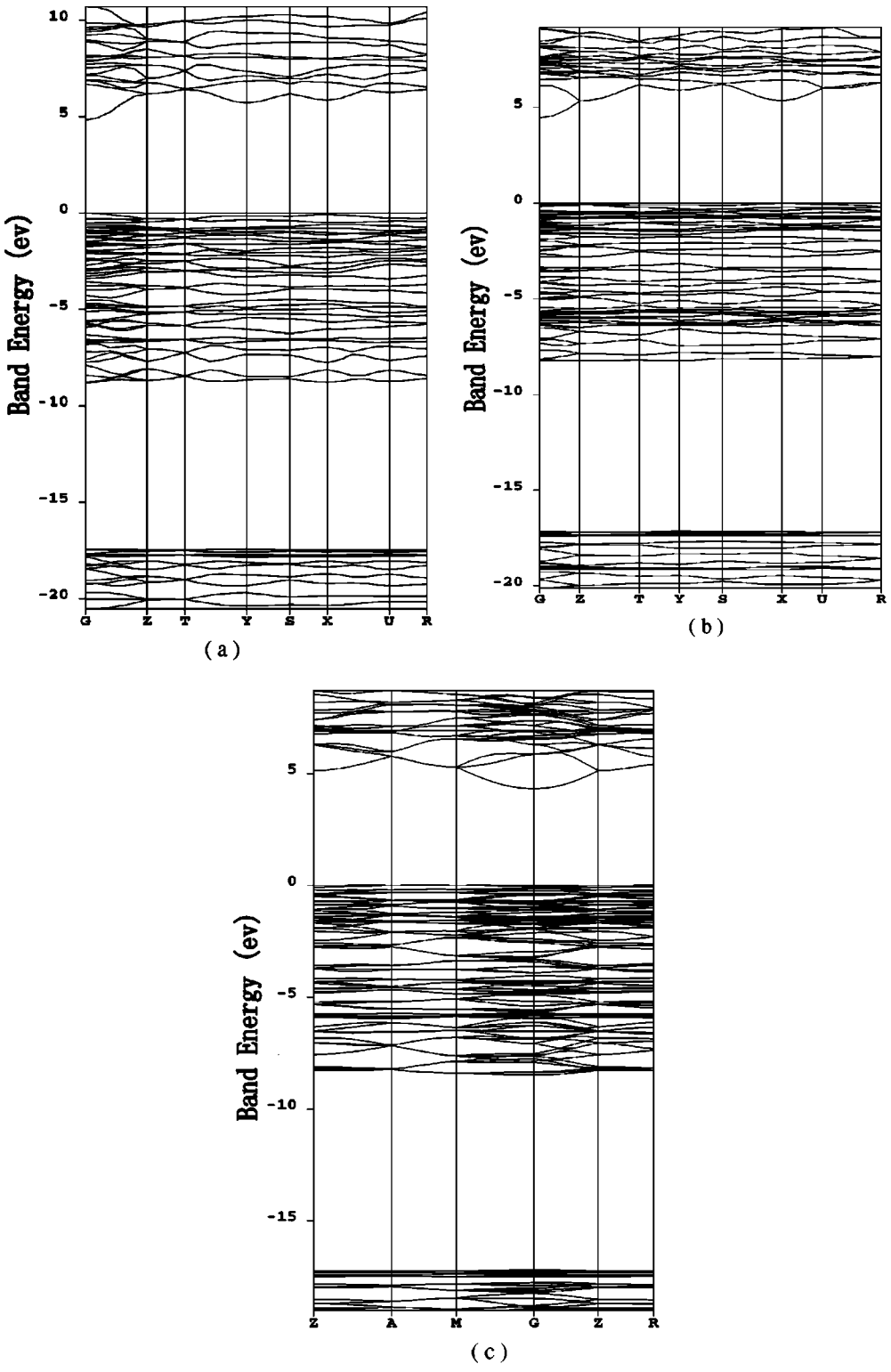


FIG. 2. Band structures of (a) LBO, (b) CBO, and (c) CLBO crystals.

absorption edges become longer, increasing from 160 to 170 and 180 nm, respectively. In fact, the above-mentioned orbital compositions of the energy bands reveal the origin of the energy-gap change. For LBO the orbitals of $Li^+$ have no contributions to either valence or conduction bands. However, for CBO and CLBO the $6p$ orbitals of Cs are inserted into the valence bands, which mainly consist of $2p$ orbitals of oxygen. It makes the valence bands increase their energy

TABLE I. Calculated and experimental band gaps of LBO, CBO, and CLBO (in eV).

| Crystal | Calculated | Experimental[a] |
|---|---|---|
| LBO | 4.825 | 7.98 |
| CBO | 4.463 | 7.26 |
| CLBO | 4.321 | 6.87 |

[a]Reference 28.

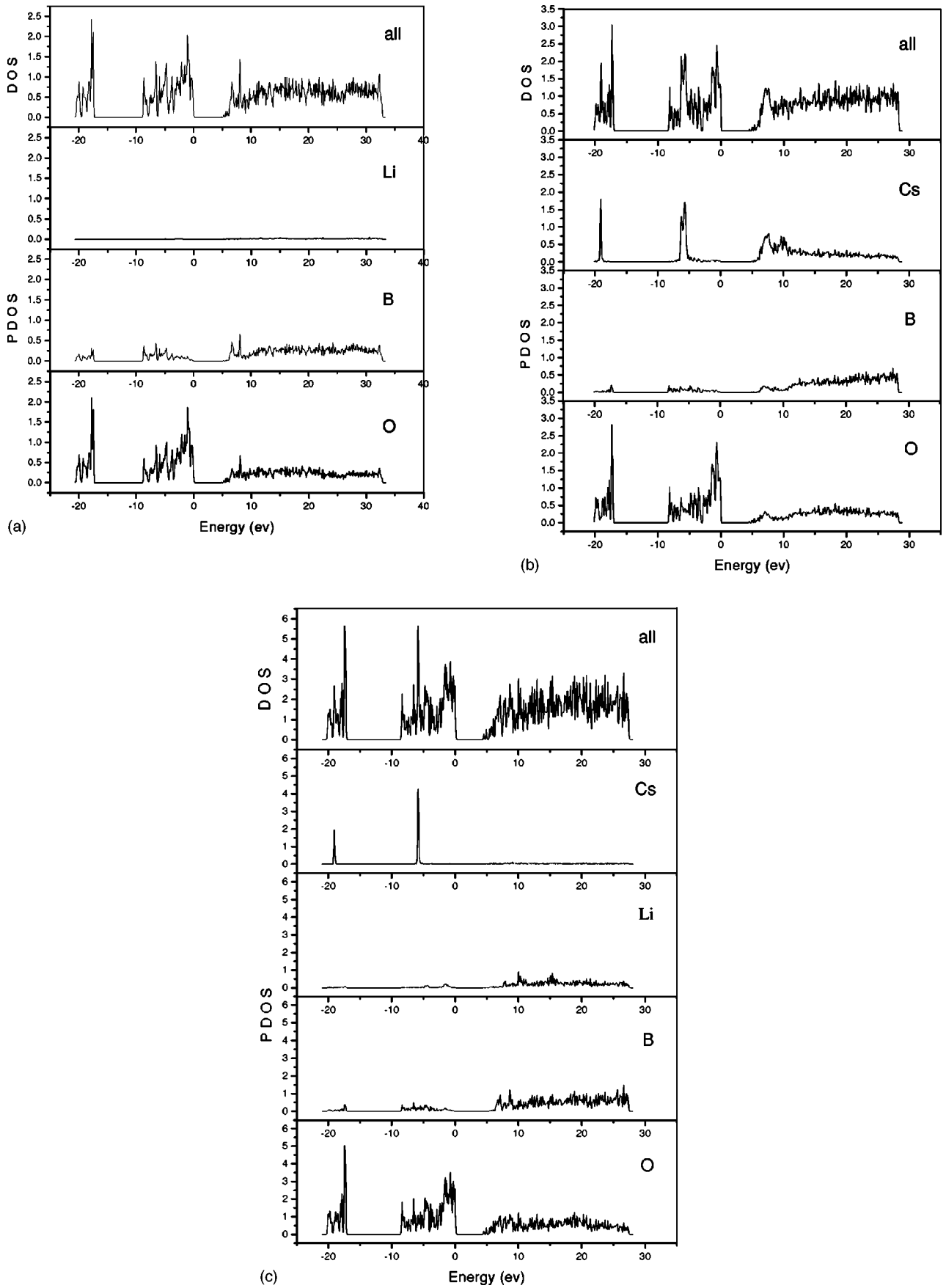


FIG. 3. Total DOS and partial DOS of (a) LBO, (b) CBO, and (c) CLBO crystals.

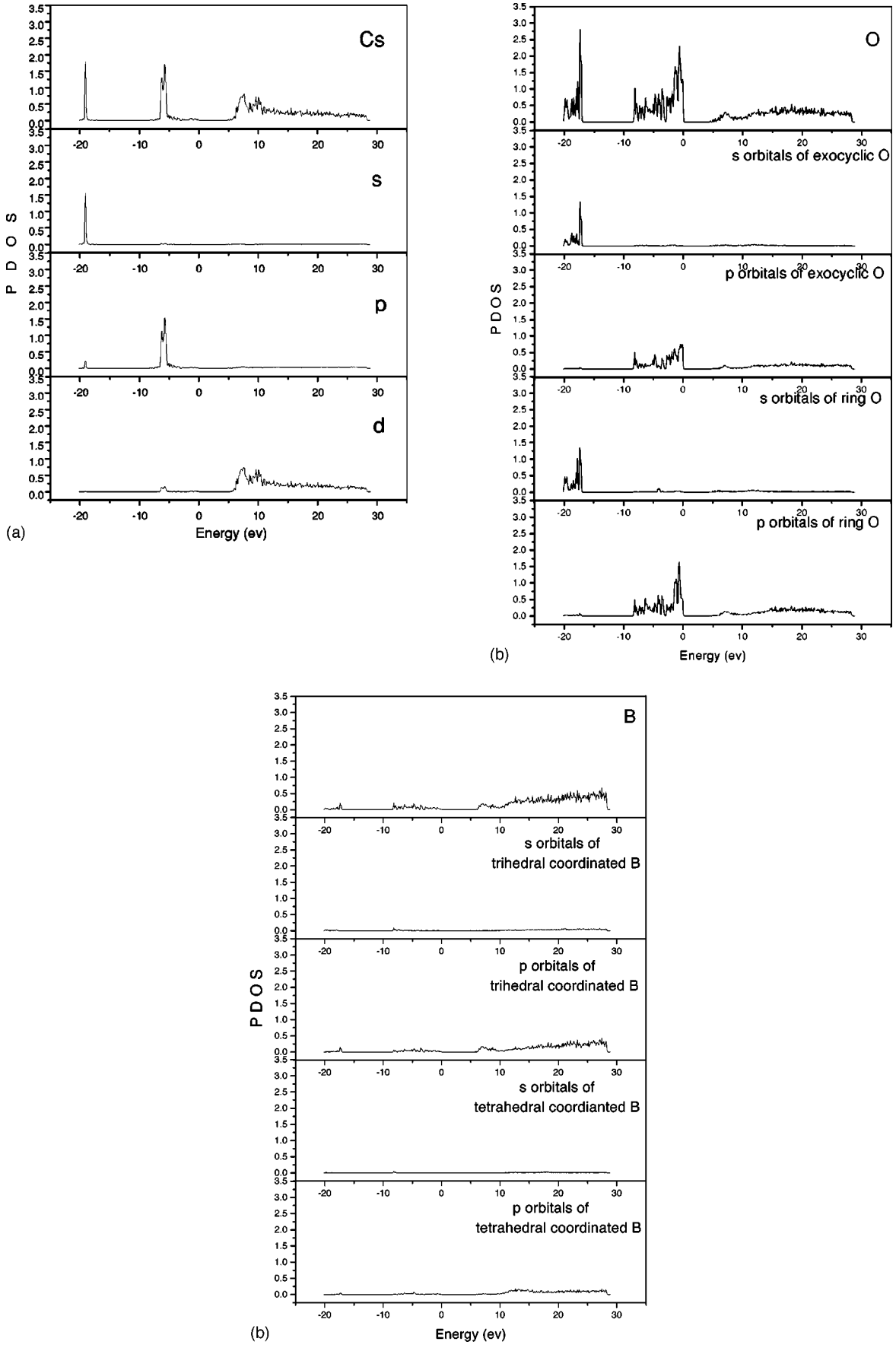


FIG. 4. Orbital-resolved PDOS of CBO (a) Cs, (b) O, and (c) B.

TABLE II. Comparison of calculated and experimental vales of refractive indexes of LBO, CBO, and CLBO at a few specific wavelengths (in $\mu$m).

| | | Experimental[a] | | | Calculated | | |
|---|---|---|---|---|---|---|---|
| Crystal | λ | $n_x$ | $n_y$ | $n_z$ | $n_x$ | $n_y$ | $n_z$ |
| LBO | 0.2537 | 1.6335 | 1.6582 | 1.6792 | 1.638 | 1.654 | 1.691 |
| | 0.3125 | 1.6097 | 1.6415 | 1.6588 | 1.615 | 1.630 | 1.666 |
| | 0.4047 | 1.5907 | 1.6216 | 1.6353 | 1.598 | 1.613 | 1.646 |
| | 0.5321 | 1.5787 | 1.6064 | 1.6212 | 1.589 | 1.603 | 1.636 |
| | 0.6563 | 1.5734 | 1.6006 | 1.6154 | 1.585 | 1.598 | 1.631 |
| | 0.8000 | 1.5696 | 1.5962 | 1.6108 | 1.582 | 1.596 | 1.628 |
| | 1.064 | 1.5656 | 1.5905 | 1.6055 | 1.580 | 1.593 | 1.625 |
| CBO | 0.3547 | 1.5499 | 1.5849 | 1.6145 | 1.602 | 1.607 | 1.640 |
| | 0.4880 | 1.5367 | 1.5736 | 1.6009 | 1.586 | 1.591 | 1.623 |
| | 0.5321 | 1.5328 | 1.5662 | 1.5936 | 1.584 | 1.588 | 1.620 |
| | 0.6328 | 1.5294 | 1.5588 | 1.5864 | 1.580 | 1.584 | 1.615 |
| | 1.0642 | 1.5194 | 1.5505 | 1.5781 | 1.573 | 1.578 | 1.608 |
| CLBO | λ | $n_o$ | $n_e$ | $\Delta n$ | $n_o$ | $n_e$ | $\Delta n$ |
| | 0.355 | 1.517 | 1.461 | 0.056 | 1.544 | 1.481 | 0.063 |
| | 0.488 | 1.501 | 1.448 | 0.053 | 1.529 | 1.468 | 0.061 |
| | 0.532 | 1.498 | 1.446 | 0.052 | 1.526 | 1.466 | 0.060 |
| | 0.633 | 1.494 | 1.442 | 0.052 | 1.522 | 1.463 | 0.059 |
| | 1.064 | 1.485 | 1.436 | 0.049 | 1.516 | 1.457 | 0.059 |

[a]References 9 and 28.

levels and reduce the band gap. Therefore, relative absorption wavelengths become longer.

### B. The linear optical susceptibilities of LBO, CBO, and CLBO

It is well known that the refractive indices are obtained theoretically from the imaginary part of the dielectric function through the Kramers-Kroning transform. The imaginary part can be calculated with the matrix elements that describe the electronic transitions in the considered crystals. The calculated formulas of the dielectric constants are given in Ref. 4. The calculated and experimental values of the refractive indices at a few wavelengths are listed in Table II. Obviously, the calculated results for the three crystals are in good agreement with the experimental values. To investigate the influence of the cation and anionic groups on the optical response of LBO, CBO, and CLBO, a real-space atom-cutting method has also been used.

In a previous paper[4] it was found that the charge density around $M$ ($M$=Li, Cs) is spherical, so we first choose the cutting radiis of Li and Cs to be 1.00 and 2.00 Å, with the same method as that in Ref. 4. Moreover, following the rule

TABLE III. Comparison of the refractive indices of LBO, CBO, and CLBO at the static limit derived from cut-$M$($M$=Li, Cs) functions and $(B_3O_7)^{5-}$ cut wave functions with original values.

| Crystal | | $n_x$ | $n_y$ | $n_z$ | $\Delta n$ ($n_{max}-n_{min}$)[a] |
|---|---|---|---|---|---|
| LBO | Total | 1.577 | 1.590 | 1.622 | 0.045 |
| | $(B_3O_7)^{5-}$ only | 1.564 | 1.578 | 1.607 | 0.043 |
| | $Li^+$ only | 1.048 | 1.052 | 1.051 | 0.004 |
| CBO | Total | 1.557 | 1.575 | 1.605 | 0.048 |
| | $(B_3O_7)^{5-}$ only | 1.360 | 1.373 | 1.414 | 0.054 |
| | $Cs^+$ only | 1.279 | 1.280 | 1.285 | 0.006 |
| Crystal | | $n_o$[b] | $n_e$[c] | | $\Delta n$ ($\lvert n_o-n_e\rvert$) |
| CLBO | Total | 1.513 | 1.455 | | 0.058 |
| | $Li^+$ only | 1.0290 | 1.0287 | | 0.0003 |
| | $Cs^+$ only | 1.125 | 1.124 | | 0.001 |
| | $(B_3O_7)^{5-}$ only | 1.419 | 1.357 | | 0.062 |

[a]$n_{max}$ is the maximal value of the refractive indices and $n_{min}$ is the minimal value of the refractive indices.
[b]$n_o$ is the refractive index of ordinary light in crystal.
[c]$n_e$ is the refractive index of extraordinary light in crystal.

TABLE IV. Comparison of calculated and experimental values of nonlinear susceptibilities of LBO, CBO, and CLBO (in pm/V).

| Crystal | $d_{ij}$ | Experimental | This work | Previous works | |
|---|---|---|---|---|---|
| LBO | $d_{31}$ | $\mp 0.67$[a] | $-0.505$ | $-0.94$[b] | 1.70[c] |
| | $d_{32}$ | $\pm 0.85$ | 0.582 | 1.04 | $-1.36$ |
| | $d_{33}$ | $\pm 0.04$ | 0.014 | 0.21 | 0.10 |
| CBO | $d_{14}$ | $\pm 1.04$[d] 0.75[b] | $-0.577$ | $-0.65$[e] | |
| CLBO | $d_{36}$ | $\pm 0.95$[f] | $-0.546$ | $-0.58$[e] | |

[a] Reference 28.
[b] Reference 29.
[c] Reference 14.
[d] Reference 30.
[e] Reference 2.
[f] Reference 9.

of keeping the cutting spheres of the cation and O in contact and not overlapped, the cutting radius of O is set to be 1.10 Å. Finally, the covalent radius 0.88 Å of B is chosen as its cutting radius in order to totally ''clear'' the electronic cloud density of the $(B_3O_7)^{5-}$ group. Our conclusions on the above calculations are the following: (i) The calculated refractive indices (see Table II) are in good agreement with the experimental values (the relative error is less than 3–5%). For CLBO, the theoretical birefringence $\Delta n$ is also in good agreement with experimental values. The agreement proves the validity of our investigation of the LBO family with the pseudopotential-based method. The results will be very helpful to NLO crystal design. (ii) Table III shows that for LBO the contributions of $Li^+$ to the refractive indices is about 10%, compared with the $(B_3O_7)^{5-}$ group, but its contribution to the anisotropy of the refractive indices can be completely neglected. For CBO the contribution of $Cs^+$ to the refractive indices is comparable to that of the $(B_3O_7)^{5-}$ group; however, its contribution to the anisotropy is still very small. Again, for CLBO the contribution of $Li^+$ and $Cs^+$ to the refractive indices is about 37% of that of the $(B_3O_7)^{5-}$ group, while its contribution to the anisotropy can also be neglected. As a result, it is worth noting that although there is some contribution to the refractive index from the cation, it has nearly nothing to do with the birefringence.

### C. SHG coefficients

According to the computational formula given in Ref. 4, the SHG coefficients of LBO, CBO, and CLBO crystals have been calculated from the band wave functions. The theoretical and experimental SHG values are listed in Table IV. In order to calculate the respective contributions of the cation and anion groups of the SHG coefficients of the three crystals, the real-space atom-cutting method is adopted again. The atom-cutting method means that if the contribution of ion $A$ to the $n$th-order polarizability is denoted as $\chi^{(n)}(A)$, we can obtain it by cutting all ions except $A$ from the original wave functions $\chi^{(n)}(A)=\chi^{(n)}$ (all ions except $A$ are cut). We have used the same atom-cutting radii as mentioned in Sec. III B. The decomposition results are given in Table V. Table V shows clearly the contributions of the $M^+$ $(M=\mathrm{Li, Cs})$ and $(B_3O_7)^{5-}$ group as well as their joint contributions. These calculated results lead to the following conclusions:

(i) Our plane-wave pseudopotential approach is suitable for studying the SHG coefficients of LBO family. We can see that the agreement of calculated and experimental values of the SHG coefficients is very well except CLBO. Concerning the $d_{36}$ of CLBO, the value calculated by both of the band-energy functions and localized molecular orbital functions is always smaller than the measured value. Therefore, the experimental value of $d_{14}$ measured by Mori *et al.*[9] is suspect. We will measure the $d_{14}$ coefficient of CLBO with a different method to test the confidence of the $d_{14}$ value in the future.

TABLE V. Analysis of the SHG coefficients using the real-space atom-cutting method (in pm/V).

| Crystal | Contributions | | | |
|---|---|---|---|---|
| | | $d_{31}$ | $d_{32}$ | $d_{33}$ |
| LBO | $Li^+$ | $-0.008$ | 0.002 | $-0.001$ |
| | $(B_3O_7)^{5-}$ | $-0.496$ | 0.571 | $-0.006$ |
| | Sum | $-0.504$ | 0.573 | $-0.007$ |
| | Origin | $-0.505$ | 0.582 | 0.014 |
| CBO | | $d_{14}$ | | |
| | $Cs^+$ | $-0.098$ | | |
| | $(B_3O_7)^{5-}$ | $-0.342$ | | |
| | Sum | $-0.440$ | | |
| | Origin | $-0.577$ | | |
| CLBO | | $d_{36}$ | | |
| | $Li^+$ | $-0.006$ | | |
| | $Cs^+$ | $-0.138$ | | |
| | $(B_3O_7)^{5-}$ | $-0.222$ | | |
| | Sum | $-0.366$ | | |
| | Origin | $-0.546$ | | |

(ii) Obviously, the contributions to the $d_{31}$ and $d_{32}$ coefficients from the anionic group $(B_3O_7)^{5-}$ go beyond 95% for LBO. These $d_{ij}$ coefficients are almost the ''pure'' contribution of the anionic group $(B_3O_7)^{5-}$. The results of the analysis of the SHG coefficients using the real-space atom-cutting method clearly show that with the increase of the radius of the metal cations $M^+$, their contributions to the larger SHG coefficients become more and more significant. For example, only 1% of the largest $d_{32}$ of LBO comes from the $Li^+$ cation; on the other hand, for CBO the contribution of the cation $Cs^+$ to the $d_{14}$ is approximately 15%.

## IV. CONCLUSION

An *ab initio* electronic band-structure calculation has been carried out using the CASTEP package to study the optical properties of LBO, CBO, and CLBO. Our investigations are summarized as follows.

(i) The electronic and band structure of CLBO has been obtained. The calculated band structure of CLBO has been compared with those of LBO and CBO. The band structures of these three crystals are qualitatively similar to each other. The DOS and PDOS figures reveal the compositions of each energy band. The tops of the VB are almost a mixture of the $p$ orbitals of the oxygen atoms. The conduction bands of the three crystals are mainly composed of valence orbitals of B and O, but for CBO there are some contributions from the $d$ orbitals of the Cs atom.

(ii) From the wave functions and band structures the linear and nonlinear optical coefficients have been obtained for the three crystals. The calculated refractive indices and SHG coefficients are in good agreement with the experimental values. On the basis of the real-space atom-cutting method, the respective contributions of cation and $(B_3O_7)^{5-}$ groups to the total optical response have been evaluated. The results show that even the contribution of the $Cs^+$ cation to the refractive indexes of CBO is comparable to that of the $(B_3O_7)^{5-}$ group, but its contribution to the anisotropy of the refractive indexes (for example, $n_{max}-n_{min}$ for LBO and CBO) can be neglected. This means that the anisotropy of the refractive indices of LBO, CBO, and CLBO is mainly determined by the $(B_3O_7)^{5-}$ group. The contributions to the SHG coefficients from the $(B_3O_7)^{5-}$ group go beyond 95% for LBO, but with the increase of the radius of cation $M^+$, their contributions to the SHG coefficients become slightly more important. For example, the contribution of the $Cs^+$ cation to the SHG coefficient is about 15% for CBO and the joint contribution of $Li^+$ and $Cs^+$ to the SHG coefficient is about half that of the $(B_3O_7)^{5-}$ group for CLBO. As a result, calculations of the SHG coefficients of LBO, CBO, and CLBO indicate clearly that the major part of the SHG coefficients for these crystals still come from the $(B_3O_7)^{5-}$ group. We believe that further applications of the real-space atom-cutting method may elucidate the origin of the optical effects, both linear and nonlinear for other NLO crystals.

## ACKNOWLEDGMENTS

This work was supported by the Chinese National Key Basic Research Project. Support in computing facilities from the Computer Network Information Center is gratefully acknowledged.

*Present address: Department of Material Science, Mailbox 138-78, California Institute of Technology, Pasadena, CA 91125.

[1] CASTEP 3.5 program, Molecular Simulation Inc., 1997.
[2] W. Kohn and L. J. Sham, Phys. Rev. **140**, A1133 (1965).
[3] R. G. Parr and W. T. Yang, *Density Functional Theory of Atom-Molecules* (Oxford University Press, Oxford, 1989).
[4] J. Lin, M. H. Lee, Z. P. Liu, C. T. Chen, and C. J. Pickard, Phys. Rev. B **60**, 13 380 (1999).
[5] C. T. Chen, Y. C. Wu and R. K. Li, Chin. Phys. Lett. **2**, 616 (1985).
[6] C. T. Chen, Y. C. Wu, A. D. Jiang, B. C. Wu, G. M. You, R. K. Li, and S. J. Lin, J. Opt. Soc. Am. B **6**, 389 (1989).
[7] Y. C. Wu, T. Sasaki, S. Nakai, A. Yokotani, H. Tang, and C. T. Chen, Appl. Phys. Lett. **62**, 2614 (1993).
[8] J. M. Tu and D. A. Keszler, Mater. Res. Bull. **30**, 209 (1995).
[9] Y. Mori, I. Kuroda, S. Nakajima, T. Sasaki, and S. Nnakai, Appl. Phys. Lett. **67**, 1818 (1993).
[10] R. H. French, J. W. Ling, F. S. Ohuochi, and C. T. Chen, Phys. Rev. B **44**, 8496 (1991).
[11] Y. N. Xu and W. Y. Ching, Phys. Rev. B **41**, 5471 (1990).
[12] Y. N. Xu, W. Y. Ching, and R. H. French, Phys. Rev. B **48**, 17 695 (1993).
[13] J. Li, C. G. Duan, Z. Q. Gu, and D. S. Wang, Phys. Rev. B **57**, 6925 (1998).
[14] C. G. Duan, J. Li, Z. Q. Gu, and D. S. Wang, Phys. Rev. B **59**, 369 (1999).
[15] C. G. Duan, J. Li, Z. Q. Gu, and D. S. Wang, Phys. Rev. B **60**, 9435 (1999).
[16] P. Perdew and Y. Wang, Phys. Rev. B **45**, 13 244 (1992).
[17] M. C. Payne, M. P. Teter, D. C. Allan, T. A. Aries, and J. O. Joannopoulos, Rev. Mod. Phys. **64**, 1045 (1992).
[18] A. M. Rappe, K. M. Rabe, E. Kaxiras, and J. D. Joannopoulos, Phys. Rev. B **41**, 1227 (1990).
[19] J. S. Lin, A. Qtseish, M. C. Payne, and V. Heine, Phys. Rev. B **47**, 4174 (1993).
[20] M-H. Lee, J-S. Lin, M. C. Payne, V. Heine, V. Milman, and S. Crampin (unpublished).
[21] L. Kleinman and D. M. Bylander, Phys. Rev. Lett. **48**, 1425 (1982).
[22] R. W. Godby, M. Schluter, and L. J. Sham, Phys. Rev. B **37**, 10 159 (1988).
[23] C. S. Wang and B. M. Klein, Phys. Rev. B **24**, 3417 (1981); M. S. Hybertsen and S. G. Louie, *ibid.* **34**, 5390 (1988).
[24] S. N. Rashkeev, W. R. L. Lambrecht, and B. Segall, Phys. Rev. B **57**, 3905 (1998).
[25] H. Konig and A. Hoppe, Z. Anorg. Allg. Chem. **439**, 71 (1978).
[26] J. Krogh-Moe, Acta Crystallogr. **13**, 889 (1960); Acta Crystallogr., Sect. B: Struct. Crystallogr. Cryst. Chem. **30**, 1178 (1974).
[27] T. Sasaki, Y. Mori, I. Kuroda, S. Nakasima, K. Yamaguch, S. Watanabe, and S. Naki, Acta Crystallogr. **51**, 2222 (1995).
[28] V. G. Dmitriev, G. G. Gurzadyan, and D. N. Nikogosyan, *Handbook of Nonlinear Optical Crystals* (Springer, New York, 1995).
[29] C. T. Chen, N. Ye, J. Lin, J. Jiang, W. R. Zeng, and B. C. Wu, Adv. Mater. **11**, 107 (1999).
[30] C. T. Chen, Y. Wang, Y. Xia, B. C. Wu, D. Y. Tang, W. L. Zeng, L. H. Yu, and L. Mei, J. Appl. Phys. **77**, 2268 (1995).